Indian Journal of Biochemistry & Biophysics
Vol. 61, November 2024, pp. 639-658
DOI: 10.56042/ijbb.v61i11.6391

Deciphering the therapeutic potential of bergenin in breast cancer: *In silico* insights into HSP90AA1 and HRAS interaction mediated inhibition of PI3K-Akt and MAPK signaling pathway

Priyesh Kumar, Khairah Ansari & Devendrasinh Jhala*

Department of Zoology, Biomedical Technology and Human Genetics,
University School of Sciences, Gujarat University, Ahmedabad-380 009, Gujarat, India

Received 06 November 2023; *revised 03 August 2024*

Despite advancements in technology and cancer therapies, breast cancer remains the primary cause of death among Indian women. Integrating phytochemicals might mitigate the side effects of the anticancer drugs. To curb disease progression and enhance treatments, studying organic compounds and plant-derived phytochemicals proves effective. This study investigates Bergenin, a bioactive compound from *Peltophorum pterocarpum* (Copperpod), using network pharmacology and molecular docking against breast cancer.

Pharmacological analysis *via* QikProp 4.4 suggests Bergenin aligns with ADME (absorption, distribution, metabolism and excretion) criteria and Lipinski's rule of five, which is a promising sign for its potential as a drug. Bergenin's protein targets, identified from ChEMBL (Chemogenomics - European Molecular Biology Laboratory), Swiss Target Prediction, and PharmMapper, were overlapped with breast cancer targets from GeneCards and PathCards. A PPI (protein-protein interaction) network was constructed from 246 shared targets, based on the STRING (Search Tool for the Retrieval of Interacting Genes/Proteins) 11.5 which reveals key targets of Bergenin for breast cancer. GO (Gene Ontology) and KEGG (Kyoto Encyclopedia of Genes and Genomes) analysis using DAVID (Database for Annotation, Visualization, and Integrated Discovery) provided functional insights. A CPDT (Compound–Pathway–Disease–Target) Network was constructed based on consolidated data, revealing 20 pathways, 8 diseases, and 161 core targets. Through cytoHubba, 17 crucial targets were pinpointed. Molecular docking indicated Bergenin's strong interactions with HSP90AA1, HRAS, and AKT1. Molecular Dynamics simulations affirmed stable interactions, suggesting potential inhibitory effects. Therefore, Bergenin could be a potential therapeutic drug to treat cancer *via* PI3K-Akt and MAPK signaling pathway.

Keywords: Breast cancer, Molecular docking, Molecular dynamics simulation, Network pharmacology, *Peltophorum pterocarpum*

Breast cancer is the most common cancer diagnosed in women and is a significant contributor to female mortality, accounting for approximately 2.3 million newly diagnosed cases, making up 11.7% of all cancer incidents, and 685,000 deaths worldwide. It has surpassed lung cancer as the leading cause of global cancer incidence in 2020[1]. It is the main cause of cancer-related morbidity and mortality in urban Indian women. As of 2020, it accounted for 39.4% of all cancers in India[2]. There are currently many accessible therapeutic methods available for breast cancer treatment, including the traditional treatments of surgical resection and radiation, as well as innovative interventional medications. Chemotherapy improves disease-free and overall survival in women with breast cancer, which depends on the treatment approach, characteristics of the tumor, comorbid conditions, age, and risk of recurrence[3]. Chemotherapy-induced short-term side effects such as nausea, vomiting, and digestive irritation and long-term side effects such as premature ovarian failure, weight gain, cardiac effect, leukemia, and cognitive dysfunction[3] lead to treatment discontinuation.

Network pharmacology is a novel science that combines bioinformatics and pharmacology to discover new medication targets by understanding the complex interactions between multiple components of a biological system, such as proteins and genes. Initially, Hopkins suggested the notion of network pharmacology in 2007. Since then, this technique has been frequently employed to develop more effective treatments for diseases[4]. Cancer is a polygenic disease, and single-target therapy is ineffective in treating cancer. The goal of network pharmacology is to convert the old "single

*Correspondence:
E-mail: ddjhala@gmail.com

drug-single target therapy" idea into a "multidrug component-multitarget treatment" approach[5]. This multidisciplinary approach has the potential to revolutionize the way we approach the treatment of complex diseases. Network-target-based network pharmacology represents a promising avenue for the future of drug research and development, particularly in the context of herbal formulations[6]. Conversely, molecular docking is a computational technique employed to forecast the binding strength between a potential small drug molecule and a specific protein target. The combination of network pharmacology, molecular docking and molecular dynamics simulation provides a powerful tool for the discovery and development of new drugs for breast cancer. By considering the complex interactions between multiple components of the disease network, network pharmacology helps to identify new therapeutic targets, while molecular docking and dynamics allows researchers to evaluate the potential of drugs to bind to these targets and modulate the network in a manner that can suppress the disease. This integrated approach can lead to the discovery of new, more effective treatments for breast cancer.

Therefore, in this study, the Compound–Pathway–Disease–Target Network was constructed to evaluate the possible mechanisms of Bergenin – a bioactive compound of *Peltophorum pterocarpum* flowers, in breast cancer prevention. Figure 1 exhibits a workflow of the research design. The Bergenin candidate genes and intersection genes for breast cancer were first gathered. The protein-protein interaction (PPI) and Compound–Pathway–Disease–Target Network were then built and analysed to examine key targets. Furthermore, Gene Ontology (GO) and the Kyoto Encyclopedia of Genes and Genomes (KEGG) analysis were carried out. Finally, molecular docking and dynamics was used to validate binding and stability of the key targets.

Materials and Methods

ADME analysis

To analyse the pharmacokinetic and pharmacological parameters of Bergenin, *in silico* ADME-related

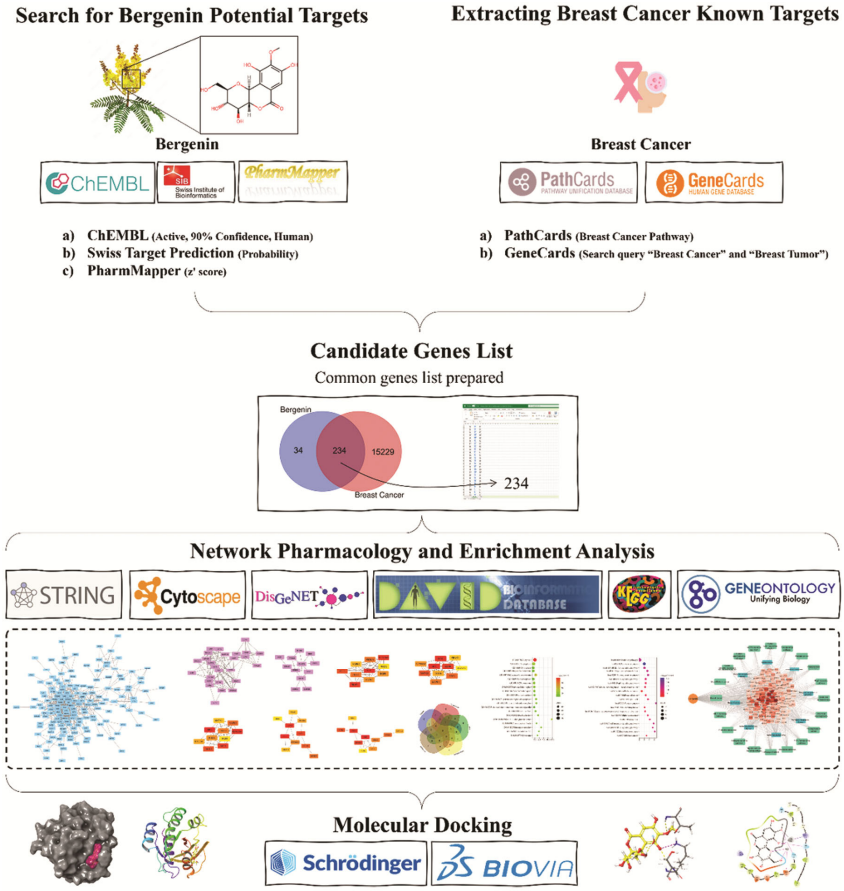

Fig. 1 — Flowchart illustrating the web tools employed for the gene selection process and its analysis for molecular docking

properties were computed using QikProp 4.4[7]. QikProp forecasts the physical descriptors and pharmaceutically important characteristics of organic compounds using absorption, distribution, metabolism, and excretion (ADME) prediction. It offers a reference range for comparing the properties of molecules to those shared by 95% of established pharmaceutical drugs. 3D structure of Bergenin was retrieved from PubChem in SDF format. To predict the pharmacokinetic characteristics of the ligand, Bergenin, the entire ADME-compliance score-drug-likeness parameter is employed. Its application predicted the octanol/water partition coefficient (QPlogPo/w), aqueous solubility (QPlogS), IC_{50} value for blockage of HERG K^+ channels (QPlogHERG), apparent Caco-2 cell permeability in nm/sec for the gut-blood barrier (QPPCaco), brain/blood partition coefficient (QPlogBB), apparent MDCK (Madin-Darby Canine Kidney) cell permeability in nm/sec (QPPMDCK), binding to human serum albumin (QPlogKhsa) and human oral absorption on 0 to 100% scale.

Preparing protein-protein interaction (PPI) network

Potential Bergenin targets and Breast cancer known targets were enumerated in order to build a protein-protein interaction network. These two lists were evaluated, and a combined list was prepared. The targets on this list were designated as candidate genes, which were utilised to construct the PPI network.

Search for bergenin potential targets

Potential targets of Bergenin were identified using online tools *viz.*, ChEMBL (active human targets at 90% confidence), PharmMapper (based on z'-score) and Swiss Target Prediction (based on probability). ChEMBL (https://www.ebi.a-c.uk/chembl/) is a database of bioactive drug-like small compounds that includes 2D structures, computed characteristics (such as Molecular weight, Lipinski parameters, logP, and so on), and abstracted bioactivities (such as ADMET data, binding constants and pharmacology). Active human targets at 90% confidence were selected as potential targets from ChEMBL[8]. PharmMapper (https://ww-w.lilab-ecust.cn/pharmmapper/) server is a free-to-use web server which detect probable target candidates for the given probe small molecules (drugs, natural products, or other recently discovered compounds with unknown binding targets). It has a high processing capacity and can quickly locate prospective target candidates in the database. PharmMapper targets were short-listed based on z' score. The calculation involves the molecule's fit score and the library score matrix. The fit score is computed by merging it with the corresponding vector from the score matrix and standardizing the result to have a mean of zero and a standard deviation of one. High positive z'-scores indicate strong target significance for a query compound, while large negative z'-scores suggest the target may lack significance. The z'-score provides more statistical significance and a highly confident comparison when added to the pure fit score[9]. Swiss Target Prediction (http://www.swisstaretpredictio-n.ch/) predicts the likely biological targets of a small molecule that is considered to be bioactive. This prediction relies on a blend of 2D and 3D similarities with a database containing over 370,000 known active compounds across more than 3,000 proteins from three different species[10].

Extracting breast cancer known targets

Already known targets of breast cancer were extracted from PathCards (https://pathcards.genecards.org/) and GeneCards (https://www.genecards.org/). PathCards is an integrated database of human biological pathways and associated annotations. Based on the commonality of the gene contents, human pathways were grouped into SuperPaths. Each PathCard holds details about a single SuperPath, which stands in for one or more human paths. It contains 1570 SuperPath entries that have been combined from 11 different sources. Genes in the superpath: "Breast Cancer Pathway" was selected. GeneCards serves as a comprehensive, user-friendly database providing detailed information on each annotated or predicted human gene. It seamlessly integrates a wide range of data types, including genomic, transcriptomic, proteomic, genetic, clinical, and functional information, sourced from approximately 150 web repositories[11]. Breast cancer known targets were extracted from GeneCards using the search queries "Breast Cancer" and "Breast Tumor".

Candidate gene list

A common list was prepared and designated as a candidate genes after removing repetitions between Potential Bergenin targets and Breast cancer known targets using Venn (https://bioinformatics.-psb.ugent.be/webtools/Venn/). The candidate gene list includes targets that are known and prospective for both breast cancer and Bergenin.

PPI-network

Protein-protein interaction network was constructed using STRING version 11.5 and Cytoscape version

3.9.1 at a confidence level of 0.9. STRING (https://string-db.org/) is a database that encompasses protein-protein interactions, encompassing both, established and anticipated interactions. These interactions originate from computational forecasts, cross-species knowledge transfer, and data collected from primary databases. They encompass direct (physical) interactions as well as indirect (functional) correlations[12]. Annotations, gene expression profiles, and various state data can be incorporated into molecular interaction networks and biological pathways through the use of the open-source software platform called Cytoscape. Cytoscape (https://cytosca-pe.org/) offers a foundational set of features for data integration, analysis, and visualisation. For network and molecular profiling analysis, new layouts, additional file format support, scripting, and connection with databases, additional capabilities are provided as apps like STRING, DisGeNET, cytoHubba and yFiles Layout Algorithm.

Core-target identification

MCODE version 2.0.2 finds clusters (highly interconnected regions) in a network. Clusters signify different things in distinct types of networks. MCODE analyze the whole PPI network and provide clusters that represent the protein complexes and parts of certain pathways[13]. The cytoHubba version 0.1, an application of Cytoscape that explores important nodes/hubs and fragile motifs in an interactome network by several topological algorithms and centralities based on shortest paths[14]. Based on Degree, Betweenness Closeness, MCC (Maximal Clique Centrality) and Bottleneck scores, top 10 targets were shortlisted, and Venn diagram was used to find the intersecting key targets.

Gene Ontology (GO) and Kyoto Encyclopedia of Genes and Genomes (KEGG) Enrichment analysis

The GO (http://geneontology.org/) knowledgebase stands as the largest global repository of gene function information. This knowledge is available in formats suitable for both human understanding and machine processing, forming a critical basis for computational analysis in the field of large-scale molecular biology and genetics experiments within biomedical research[15]. A database resource, KEGG (https://www.genome.jp/kegg/) is for understanding high-level biological system functions and utilities from molecular-level information, particularly large-scale molecular datasets produced by genome sequencing and other high-throughput experimental technology[16]. GO and KEGG pathway analysis was performed using Database for Annotation, Visualization, and Integrated Discovery (DAVID 2021)[17] (https://david.ncifcr-f.gov/) based on p-value and number of targets associated with GO and KEGG terms. DAVID offers a range of functional annotation tools to comprehend the biological significance of huge lists of genes. The bubble chart was plotted with the help of SR plot (https://www.b-ioinformatics.com.cn/en) a free online platform for data analysis and visualization.

Compound-Pathways-Disease-Target (CPDT) Network

The CPDT network was constructed by combining data from DisGeNET (https://www.disgenet.org/), the PPI network and the KEGG pathway. Disease enrichment data was extracted using Cytoscape through the DisGeNET database[18] and scrutinize gene-disease associations based on the number of target genes and p-value. Eight significant gene-disease associations were separated from DisGeNET enrichment data. Afterwards, KEGG pathway data extracted from DAVID and top 20 significant gene pathway associations based on target count were imported into Cytoscape to construct a network. The networks were then merged with the PPI network to assemble Compound-Pathways-Disease-Target Network. Cytoscape tools such as the yFiles layout algorithm and visual style were used to establish alternative symbolising identities and improve the visual features of the network.

Molecular docking

Molecular docking was performed using Schrödinger[9]. The Ligand 2D structure of Bergenin (CID 66065) was imported using canonicalsmiles provided by PubChem (https://pubchem.ncbi.nlm.nih.gov/). The imported ligand was prepared using LigPrep tool[9] and converted to a 3D structure at a pH of 7.4±0.2, including stereo chemical, ionisation, tautomeric variations, optimised for geometry, desalted and corrected for chiralities, and energy minimization using OPLS_2005 (Optimized Potentials for Liquid Simulations) force field. The key targets that underwent short listing *via* cytoHubba were utilized for the docking process. High-resolution (<2.0), non-mutated 3D structure of SRC (2bdf), HSP90AA1 (4nh8), PIK3R1 (1h9o), AKT1 (3o96), HRAS (5p21) and EGFR (6p8q) were obtained from the Protein Data Bank (PDB) (https://www.rscb.org). Protein 3D structures were prepared using Protein preparation wizard[7] at pH 7.4±2.0, where hydrogen atoms were added, hetero-molecules and water molecules were removed, and charges and bond orders were applied. PROPKA was used to optimize the structure, and

finally, the OPLS_2005 force field was applied to conduct restricted minimization of the protein structure. Further water molecules were removed at 5 Å from the ligand, and energy was reduced at a Root Mean Square Deviation (RMSD) tolerance of 0.3 Å. Receptor Grid generation was utilised to prepare a grid box at the active site of the protein. Amino acids resembling active sites of proteins were identified from Computed Atlas of Surface Topography of proteins (CASTp) (http://sts.bioe.uic.edu/castp/index.html), which recognizes pockets as empty concavities on a protein surface into which solvent can gain access based on computational geometry[19]. Leading six proteins scrutinized through cytoHubba analysis were employed for molecular docking using the Glide XP (Extra precision) method. Glide looks for favourable interactions and binds flexible ligands into stiff receptor structures. The Glide XP method incorporates a substantially broader exploration of molecular poses and employs a scoring function that rigorously assesses interactions between proteins and ligands[20]. Based on the Glide score (kcal mol^{-1}), the efficacy of ligand-protein binding was ultimately evaluated.

Molecular dynamics (MD) simulation

A 100 nanoseconds molecular dynamics simulation was conducted using the Desmond software on two primary target proteins, HSP90AA1 (4nh8) and HRAS (5p21), with a focus on their Glide scores, which indicate a more favourable binding affinity when displaying a more negative value[9]. The OPLS_2005 force field was utilised to simulate water molecules using a predefined TIP3P water model[21]. Orthorhombic periodic boundary conditions were established to define the dimensions and proportions of the repeated unit, with a buffer of 10 Å separation. To achieve electrical neutrality, seven Na^+ ions were introduced to counterbalance the system's charge. After introducing the necessary counter-ion, 0.15 M NaCl was supplied to maintain isosmotic condition in the simulation box. The Bergenin-4nh8 system had solvated box volume of 278238 $Å^3$ contained 26272 protein atoms with 7644 water molecules, while the Bergenin-5p21 system had solvated box volume of 218118 $Å^3$ comprised 20280 protein atoms with 5861 water molecules. The system was then minimised and relaxed using the Desmond module's default protocol and the OPLS_2005 force field. Coulombic interactions cut-off was set to a 9.0 Å radius. The system was developed in isothermal-isobaric ensemble NPT with a relaxation time of 1 ps and a time step of 2 fs. The Nose-Hoover chain[22] and the Martyna-Tobias-Klein isotropic scaling[23] approach was used to adjust the temperature 300.0 K and pressure 1 bar, respectively. The Simulation Interaction Diagram tool in the Desmond package was used to investigate the behaviour and interactions of the ligand with protein. RMSD and RMSF (root mean square fluctuation) plots, as well as protein-ligand interaction patterns, were analysed to examine the stability of MD simulations.

Results

ADME analysis

Drug-like properties of the compound were assessed by evaluating their pharmacokinetics and pharmacological properties using QikProp. The properties as shown in Table 1 like, molecular weight <500 Da; hydrogen bond donors <5, hydrogen bond acceptors <10, and logP values of <5, are all well withinthe acceptable range of Lipinski's rule of five[24]. ADME showed results with median to high values for human oral absorption, Caco-2 cell permeability with 46.32% absorption and 39.27 nm/sec, respectively. Predicted MDCK cell permeability was poor at 14.95 nm/sec, below the recommended value of 25 and the Brain/blood partition coefficient was found low (Table 1). The pharmacokinetic parameters fall comfortably within the acceptable range prescribed for human application, suggesting the potential of this molecule as a drug candidate.

Protein-protein interaction (PPI) network

A total of 268 targets that interact with Bergenin were found, 232 of which were obtained from PharmMapper, 23 from Swiss target prediction and 13 from ChEMBL. A total of 15,663 breast cancer-associated targets were retrieved, of which, 200 were from the "Breast cancer pathway" PathCards and 15,463 from GeneCards. 234 overlapping targets were imported into Cytoscape 3.9.1 software to construct a PPI network using STRING 11.5 database. Significantly interacting targets were shortlisted at a Confidence score of 0.90 after removing free nodes. There are 161 nodes, which represent targets and 594 edges representing interactions between those targets (Fig. 2A).

Core-target identification

Chief two PPI clusters signifying major pathways were extracted with the help of the MCODE algorithm in Cytoscape. Figure 2B illustrates that the cluster (26 nodes and 101 edges) included AKT1, CDK2, CCNA2,

Table 1 — Pharmacokinetics and pharmacological properties of Bergenin using QikProp

Sr. No.	Property/Descriptor	Bergenin	Permissible limit
1	Rule of Five[a]	0	0-4
2	CNS[b]	-2	–2 (inactive), +2 (active)
3	mol_MW[c]	328.275	130.0 – 725.0
4	donorHB[d]	5	0.0 – 6.0
5	accptHB[e]	12.05	2.0 – 20.0
6	QPlogPo/w[f]	-1.564	-2.0 – 6.5
7	QPlogS[g]	-1.711	-6.5 – 0.5
8	QPlogHERG[h]	-3.707	concern below –5
9	QPPCaco[i]	39.273	<25 poor, >500 great
10	QPlogBB[j]	-2.031	-3.0 – 1.2
11	QPPMDCK[k]	14.953	<25 poor, >500 great
12	QPlogKhsa[l]	-0.931	-1.5 – 1.5
13	Percent Human Oral Absorption[m]	46.321	>80% high, <25% poor
14	PSA[n]	157.841	7.0 – 200.0

a Number of violations of Lipinski's rule of five.
b Predicted central nervous system activity on a –2 (inactive) to +2 (active) scale.
c Molecular weight of the molecule.
d Estimated number of hydrogen bonds that would be donated by the solute to water molecules in an aqueous solution.
e Estimated number of hydrogen bonds that would be accepted by the solute from water molecules in an aqueous solution.
f Predicted octanol/water partition coefficient.
g Predicted aqueous solubility, log S. S in mol dm^{-3} is the concentration of the solute in a saturated solution that is in equilibrium with the crystalline solid.
h Predicted IC_{50} value for blockage of HERG K^+ channels.
i Predicted apparent Caco-2 cell permeability in nm/s. Caco2 cells are a model for the gut-blood barrier.
j Predicted brain/blood partition coefficient.
k Predicted apparent MDCK cell permeability in nm/s. MDCK cells are considered to be a good mimic for the blood-brain barrier.
l Prediction of binding to human serum albumin.
m Predicted human oral absorption on a 0 to 100% scale. The prediction is based on a quantitative multiple linear regression model. This property usually correlates well with Human Oral-Absorption, as both measure the same property.
n Van der Waals surface area of polar nitrogen and oxygen atoms.

and HSP90AA1 as its key targets, whilst another cluster in (Fig. 2C) (12 nodes and 19 edges) had MTOR and PIK3CA. The targets such as AKT1, HSP90AA1, and PIK3CA indicates that the PPI network holds the PI3k-Akt and mTOR pathways. Then, five algorithms *viz.*, degree, maximal clique centrality (MCC), closeness, betweenness and bottleneck in cytoHubba plug-in were used to analyse the PPI network (Fig. 3A-3E). Table 2 shows the top targets, SRC, HSP90AA1, and AKT, based on cytoHubba scoring. Based on these results, intersecting targets (Fig. 3F) were scrutinized for molecular docking.

Gene ontology (GO) and Kyoto encyclopedia of genes and genomes (KEGG) Enrichment analysis

The enrichment analysis was performed using the DAVID database to examine the biological function of candidate targets. GO enrichment analysis classified the candidate target genes in biological processes (BPs), cellular components (CCs), and molecular functions (MFs) while KEGG enrichment analysis described the involvement of candidate target genes in different signaling pathways. The size of the dot in Figure 4 reflects the number of targets associated with that term, the colour denotes -log10 (p-value), and the enrichment at the x-axis displays the ratio of the number of target genes associated with all annotated genes found in the term/pathway. KEGG enrichment (Fig. 4A) highlighted the involvement of candidate target genes in hsa01100: metabolic pathways; hsa05200: pathways in cancer and hsa04151: PI3K-Akt signaling pathway *etc*. There were 20 significantly enriched BPs (Biological Processes) terms ($P< 0.01$), with signal transduction GO: 0007165, protein phosphorylation GO: 0006468, and negative regulation of apoptotic process GO: 0043066 ranking first (Fig. 4B). GO molecular function (Fig. 4C) revealed that Protein binding GO: 0005515, identical protein binding GO:0042802, ATP binding GO: 0005524, protein homodimerization GO:0042803 are the main activities related to the target genes. Cellular components (Fig. 4D) showed that the target genes were mainly distributed in the cytosol GO: 0005829, cytoplasm GO: 0005737, nucleus GO: 0005634 and plasma membrane GO: 0005886.

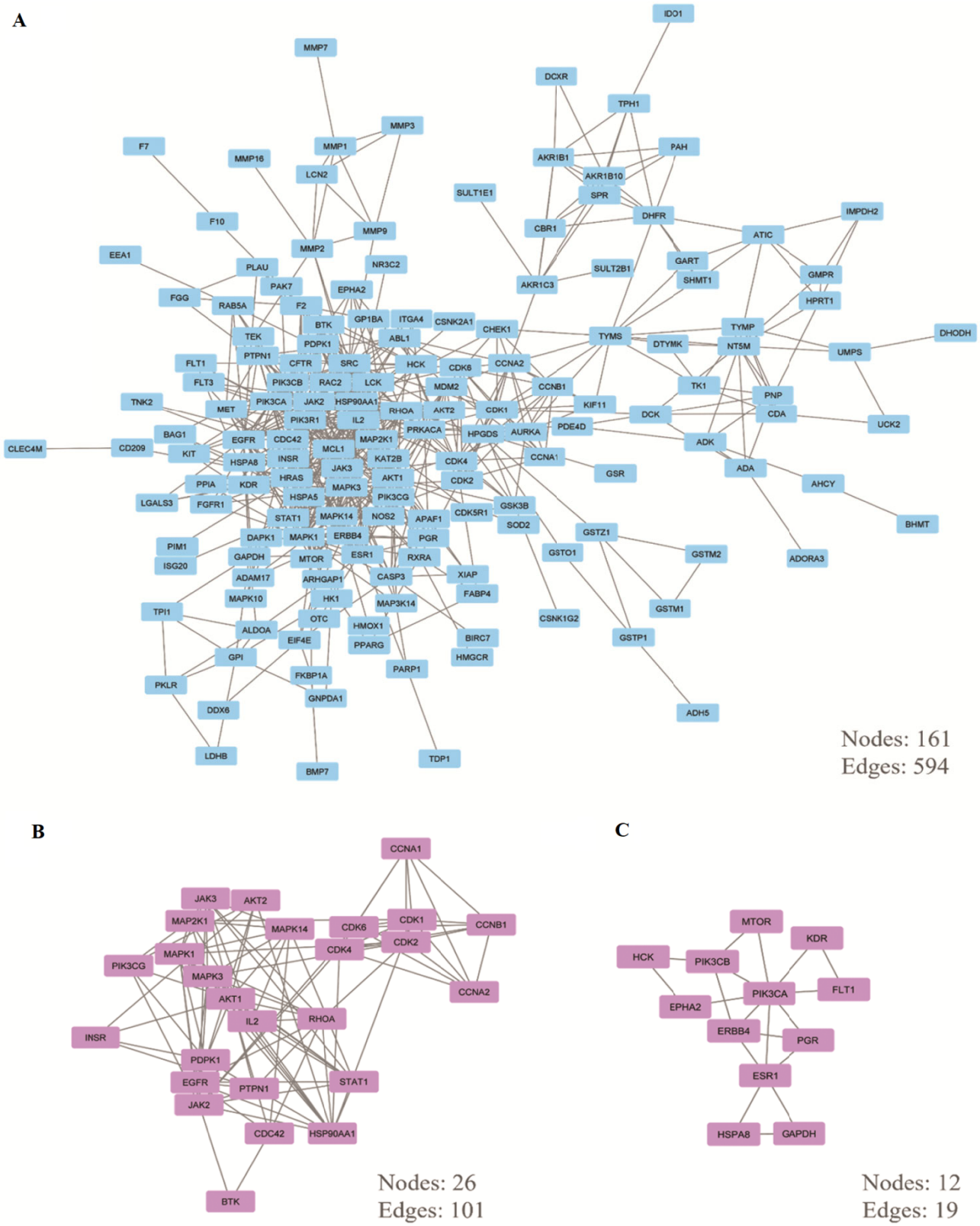

Fig. 2 — (A) PPI (Protein-Protein Interaction) network of all the possible targets of Bergenin; (B) MCODE Cluster 1; and (C) MCODE Cluster 2

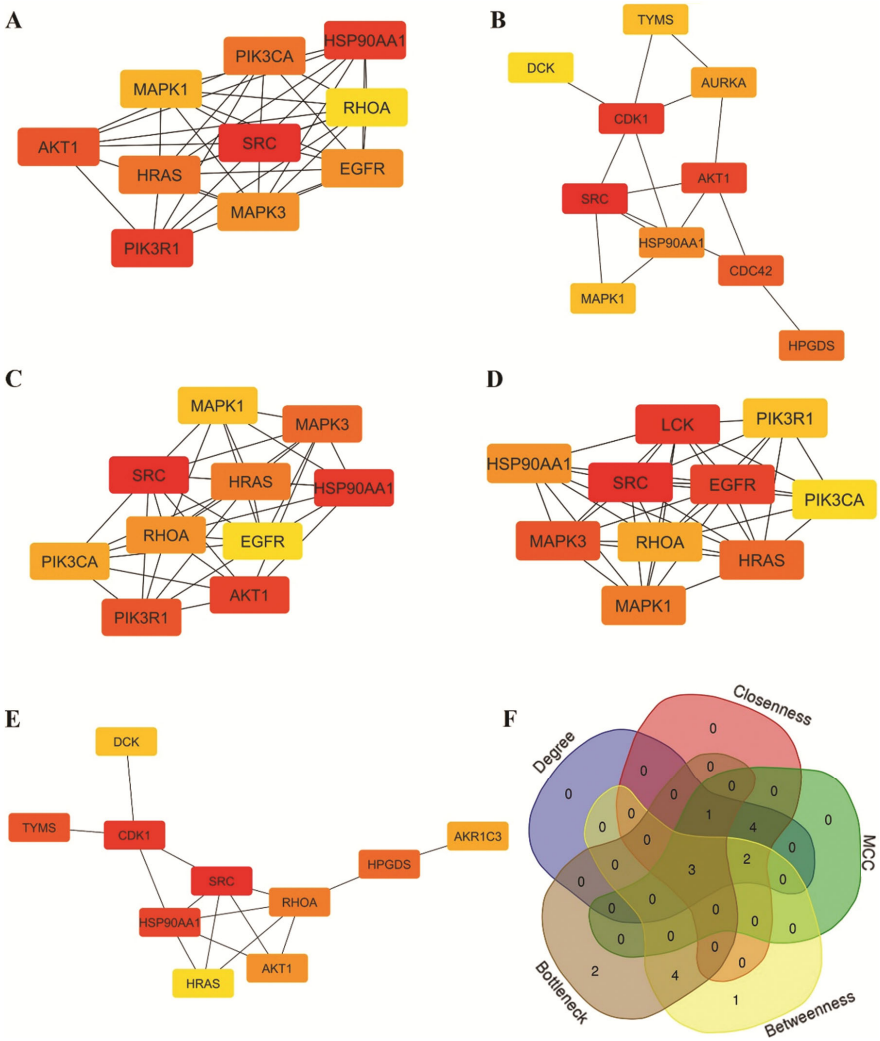

Fig. 3 — Clusters of top 10 targets in cytoHubba algorithm using Cytoscape (A) Degree; (B) BottleNeck; (C) MCC; (D) Closeness; (E) Betweenness; and (F) Intersection targets using Venn diagram

Table 2 — Top target list, cytoHubba result of Maximal Clique Centrality (MCC), Betweenness Closeness Degree and BottleNeck

Sr. No.	Targets	Degree	Closeness	MCC	Betweenness	BottleNeck
1	SRC	40	88.03333	27944	4326.860399	52
2	HSP90AA1	35	85.61667	17958	4071.533156	15
3	PIK3R1	35	81.45	17226		
4	AKT1	34	84.1	6761	2616.898129	28
5	HRAS	31	79.03333	21831	1775.198048	
6	PIK3CA	31	78.78333	16782		
7	MAPK3	27	79.11667	23063		
8	EGFR	27	77.61667	25160		
9	MAPK1	26	78.03333	21552		13
10	RHOA	25	79.01667	17467	3350.695846	
11	DCK				1790.057343	12
12	CDK1				4248.320984	32
13	HPGDS				3853.529095	16
14	TYMS				4002.467947	13
15	AKR1C3				1917.362428	
16	AURKA					14
17	CDC42					17

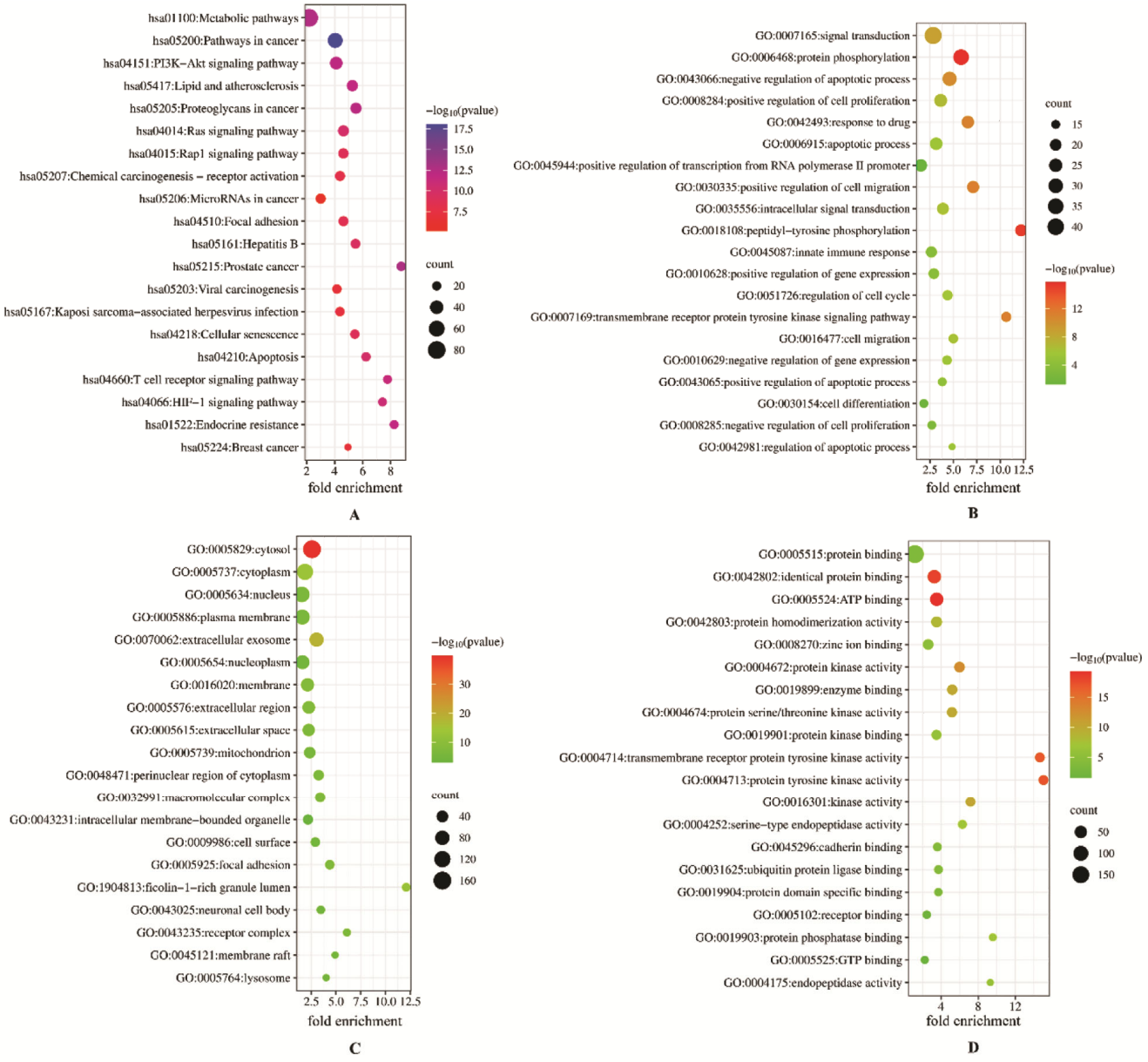

Fig. 4 — Bubble plot (A) KEGG enrichment; (B) GO Biological processes; (C) GO Cellular Components; and (D) GO Molecular Functions

Compound-pathways-disease-target (CPDT) network

The CPDT network with 190 nodes and 1892 edges (Fig. 5) as described in (Table 3) encompasses one compound, 20 pathways, 8 diseases and 161 target genes. Bergenin from the *P. pterocarpum* flower is represented by the orange round node; green nodes stand for 20 significant signaling pathways; blue nodes are 8 diseases; and red square nodes stand for 161 target genes, with lines being the interactions between them. The outermost circle of 20 KEGG pathways in green illustrates the involvement of target genes in many different essential signalling pathways such as PI3K-Akt, Breast cancer, Ras, MAPK, *etc*. The inner circle in blue depicts disease relatedness based on the number of target genes and p-value, which includes malignant neoplasm of the breast (1.50E-10), breast carcinoma (1.48E-18), schizophrenia (6.61E-10) mammary neoplasms, human (1.79E-16), mammary neoplasms (2.04E-16), mammary carcinoma, human (1.79E-16), prostatic neoplasms (1.00E-10)and malignant neoplasm of prostate (1.00E-10) (Table 4). According to DisGeNET disease relatedness statistics, the group of target genes is significantly correlated with Breast cancer. The CPDT network study

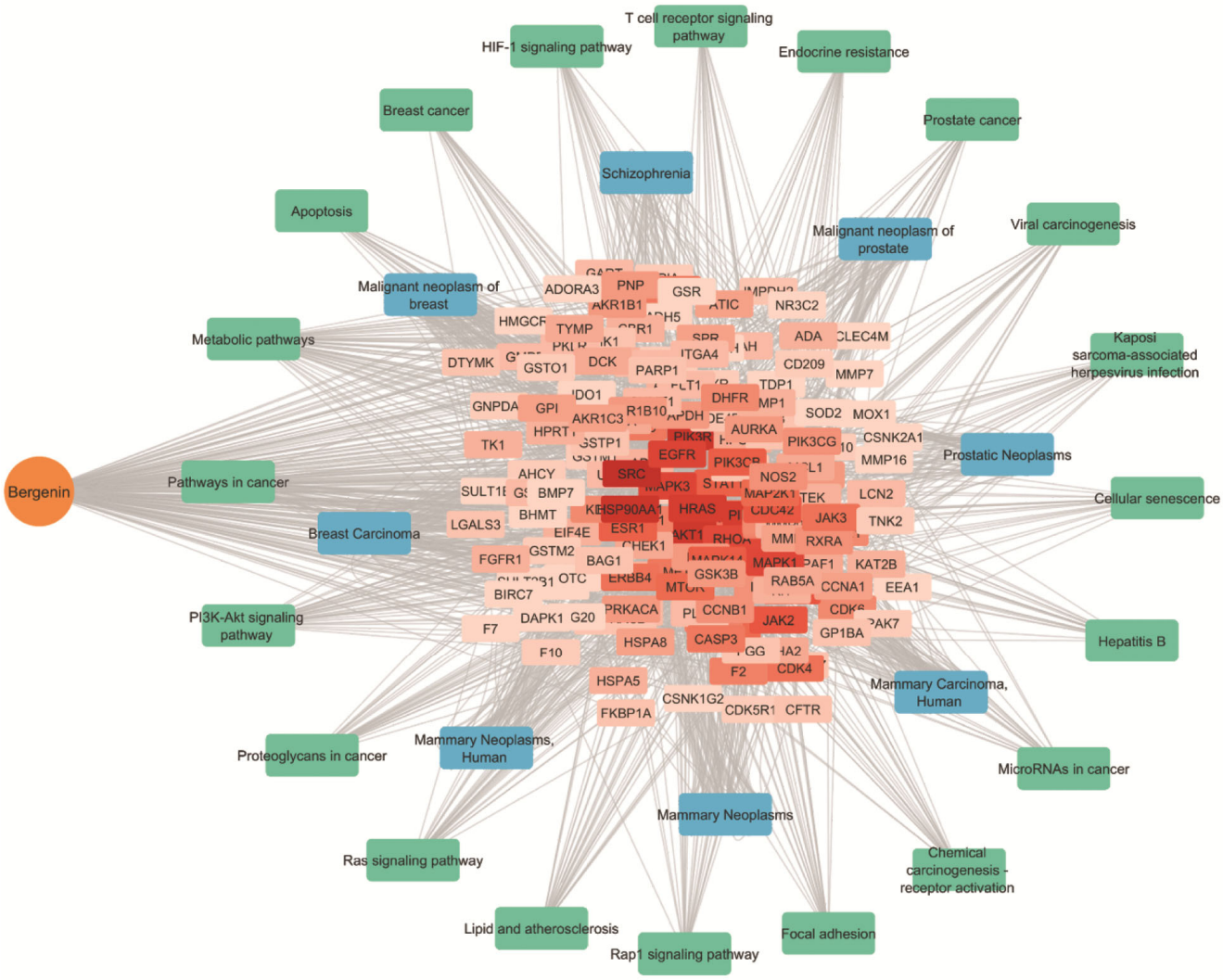

Fig. 5 — Compound-Pathways-Disease-Target Network (CPDT)

Table 3 — CPDT components with nodes and edges

Components	Nodes	Edges
KEGG Pathways	20	488
STRING genes	161	594
DisGeNET Diseases	8	650

Table 4 — DisGeNET diseases based on number of target genes involved

Sr. No.	Disease name	No. of genes	p-value
1	Malignant neoplasm of breast	46	1.50E-10
2	Breast Carcinoma	42	1.48E-18
3	Schizophrenia	40	6.61E-10
4	Mammary Neoplasms, Human	39	1.79E-16
5	Mammary Neoplasms	39	2.04E-16
6	Mammary Carcinoma, Human	39	1.79E-16
7	Prostatic Neoplasms	34	1.00E-10
8	Malignant neoplasm of prostate	34	1.00E-10

identified several proteins as significant targets, including SRC, HSP90AA1, PIK3R1, AKT1, HRAS, PIK3CA, MAPK3, and EGFR, as key targets of Bergenin in cancer treatment. These targets have the potential to affect various cancer-related pathways, including the PI3K-Akt signaling pathway, proteoglycans in cancer, Ras signaling pathway, apoptosis, prostate cancer and breast cancer, and hence offer promise for future cancer treatment.

Molecular docking

A total of six core target proteins were selected for molecular docking based on cytoHubba inspection. A more negative Glide score means more favourable protein-ligand interactions. Molecular docking results in Table 5 demonstrated that Bergenin has the best Glide score with SRC, PIK3R1, AKT1, HRAS, and

Table 5 — Molecular docking results of selected proteins with Bergenin compared docking of with FDA approved drugs

Sr. No.	Targets (PBD ID)	Positive Inhibitor	Bergenin		
		Glide gscore (Kcal/mol)		Hydrogen bond interactions (Å)	Interacting Amino Acids
A	SRC (2BDF)	-4.857	-7.214	GLU280 (1.71127), ASP258, TYR335, LYS316	PRO299, LYS298, THR296, PRO333, LYS315, GLN312, LEU269, TRP282, ALA259, TRP260, GLN275
B	HSP90AA1 (4NH8)	-8.227	-12.071	LEU103 (1.63734),ASN51, GLY135	MET98, VAL150, ASP102, OLE104, PHE22, PHE170, ASN105, LEU107, GLY108, TRP162, ALA111, VAL136, PHE138, TYR139
C	PIK3R1 (1H90)	-1.655	-7.321	ARG19 (1.5915), ARG37, HIS57, SER40	ARG37, ASN18, SER39, LYS41, ALA46, VAL59, CYC58
D	AKT1 (3O96)	-1.819	-9.954	GLU278 (1.75583), ASN279, GLU298, PHE293	TYR229, VAL164, LEU156, GLY157, THR291, GLY294, LEU295, ASP274, LYS276, MET281, GLU234
E	HRAS (5P21)	-3.053	-11.570	SER17 (2.62482), THR35, HOH	ALA18, GLY15, GLY13, GLY12, THR58, ALA59, GLN61, THR35, PRO34, TYR32, ASP30, VAL29
F	EGFR (6P8Q)	-4.026	-9.585	ASP837 (1.66635)	VAL726, LEU718, GLY719, SER720, GLY721, ALA722, ARG841, ASN842, PRO877, ASP855

EGFR of -7.214, -7.321, -9.954, -11.570 and -9.585, respectively, compared to the standard FDA authorised medications Dasatinib (-4.857), Alpelisib (-1.655) Idealisib (-1.819), Tipifarnib (-3.053), and Gefitinib (-4.026). Bergenin concomitantly binds to HSP90AA1 with the best glide score (-12.071) compared to the standard FDA-approved drug Irsogladine (-8.227). Figure 6 reveals that Bergenin docked at a key binding pocket of proteins at different binding modes in the active site forming H-bonds, ionic bonds and π – π interactions. Moreover, Bergenin interacts with Mg^{++} of HRAS and EGFR to form metal acceptor connections (Fig. 6A-6F).

Molecular dynamics (MD) simulation

The protein-ligand complex with the highest Glide score was chosen for MD simulation to investigate the stability, conformational changes, and underlying molecular interactions at the atomic level. The behaviour and stability of docked complexes, Bergenin-4nh8 and Bergenin-5p21, i.e., Bergenin with HSP90AA1 and with HRAS respectively, were shown *via* a real-time simulation trajectory of 100 ns. Plot in (Fig. 7A & B) exhibits the protein ligand RMSD evolution with protein C-α atoms (left axis) of Bergenin-4nh8 and Bergenin-5p21 complex respectively. System was equilibrated perfectly since the structural conformation throughout the simulation remains stable. Up to 35 ns, initial fluctuations in the acceptable range of 1.0 - 3.0 Å of Bergenin-4nh8 were observed, followed by stabilization at 2.4 Å from 35 to 100 ns. While the Bergenin-5p21

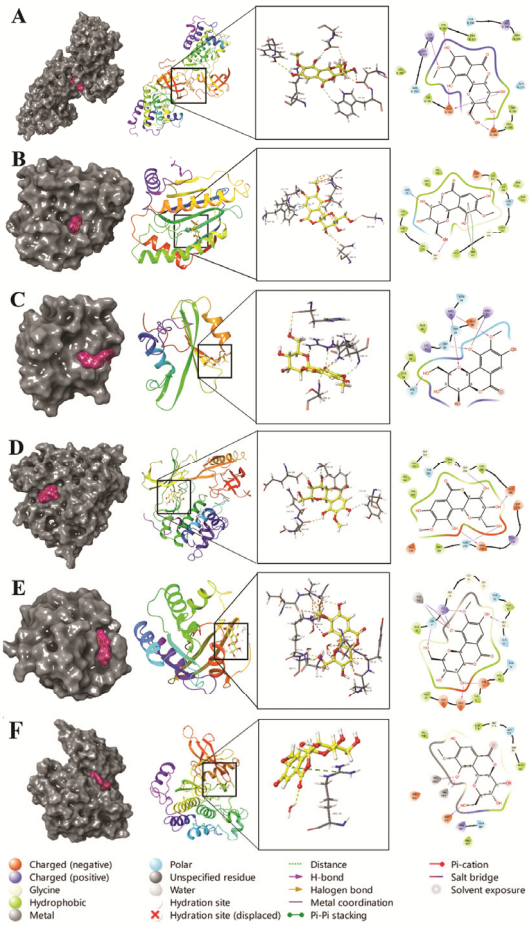

Fig. 6 — 3-D and 2-D Diagrammatic representations of Bergenin docked with different proteins (A) SRC (2BDF); (B) HSP90AA1 (4NH8); (C) PIK3R1 (1H9O); (D) AKT1 (3O96); (E) HRAS (5P21); and (F) EGFR (6P8Q)

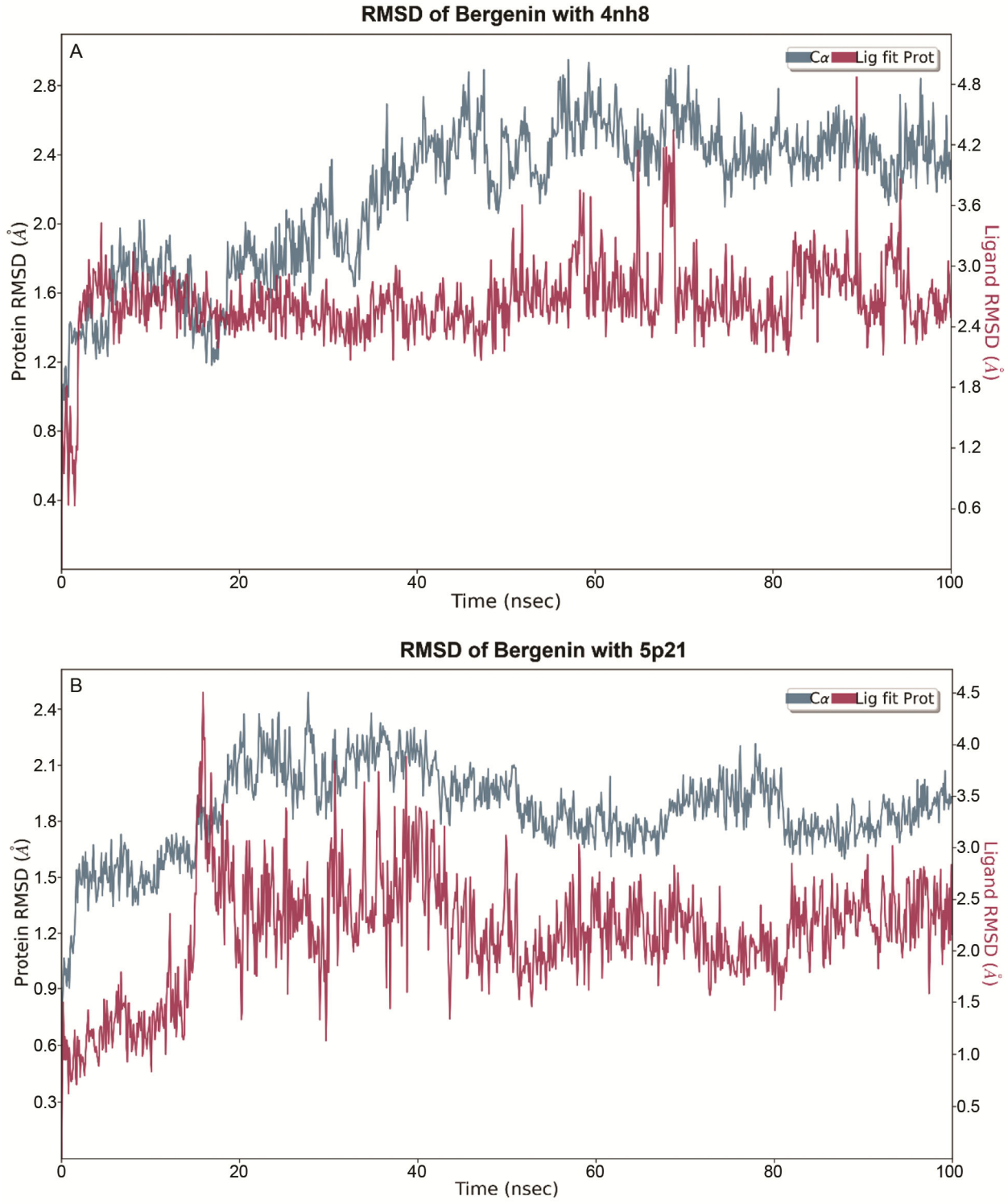

Fig. 7 — Protein and Ligand Root Mean Square Deviation (RMSD) of (A) 4nh8 with Bergenin; and (B) 5p21 with Bergenin

system oscillates for up to 40 ns from 1.0 to 2.4 Å and then stabilizes after 40 ns between 3.0 to 4.0 Å. Ligand RMSD (right axis) reveals the stability of Bergenin with respect to protein in its binding pocket. Bergenin simulated with 4nh8 attain stability after 4 ns and remains steady between 2.0 to 3.5 Å from 5 to 100 ns, whereas ligand RMSD of 5p21 initially fluctuates alike C–α of protein up to 40 ns and then

remains stable between 2.0 to 3.0 Å. Figure 8A and 8B depicts protein RMSF of Bergenin-4nh8 and Begrenin-5p21 as local variations along the protein chain that fluctuate less at rigid secondary structures such as alpha helices and beta strands. In Figure 8A, ligand connections were depicted by green lines, suggesting that ligand contacts formed at stable secondary conformations of 4nh8 with variations less

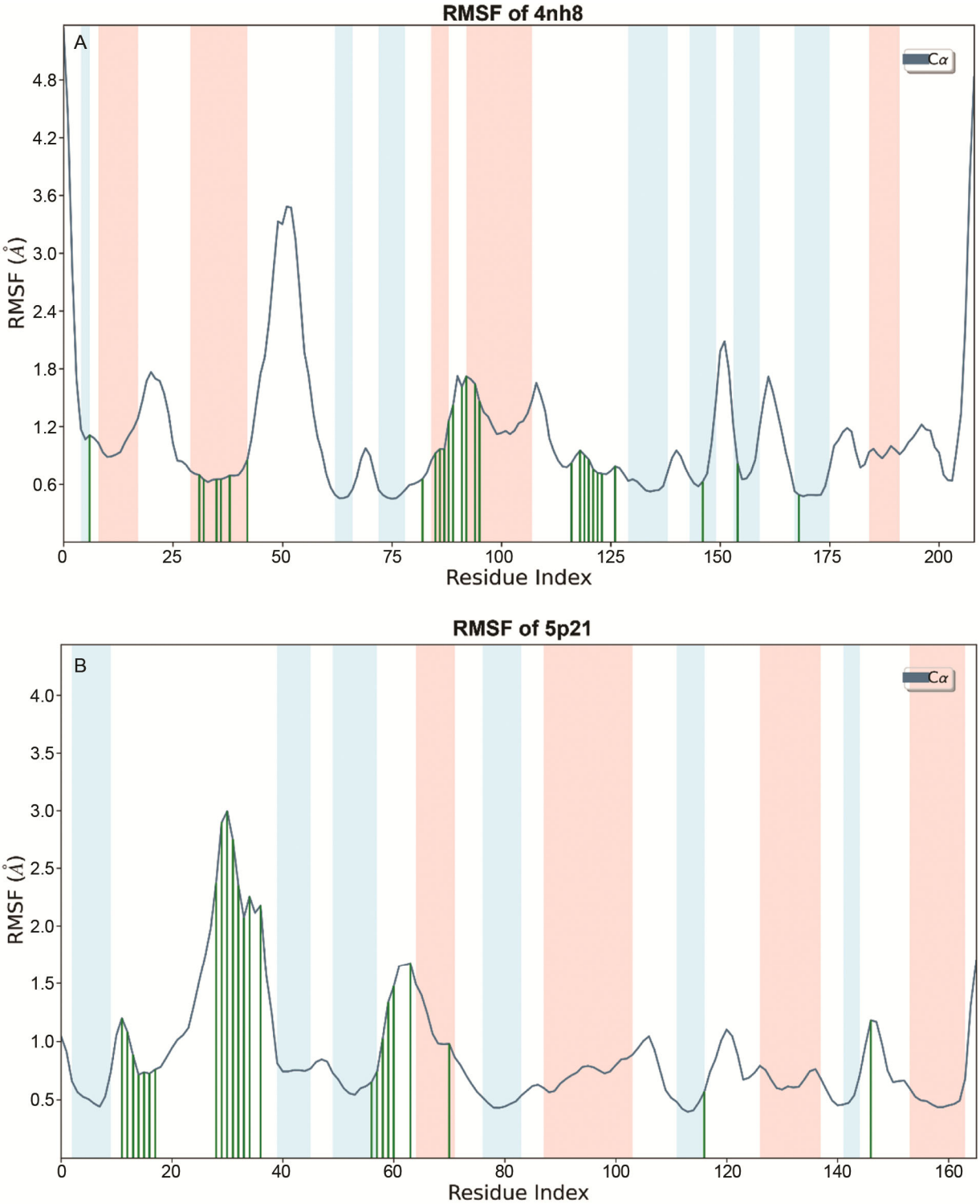

Fig. 8 — Protein Root Mean Square Fluctuation (RMSF) with interacting residues of (A) 4nh8; and (B) 5p21

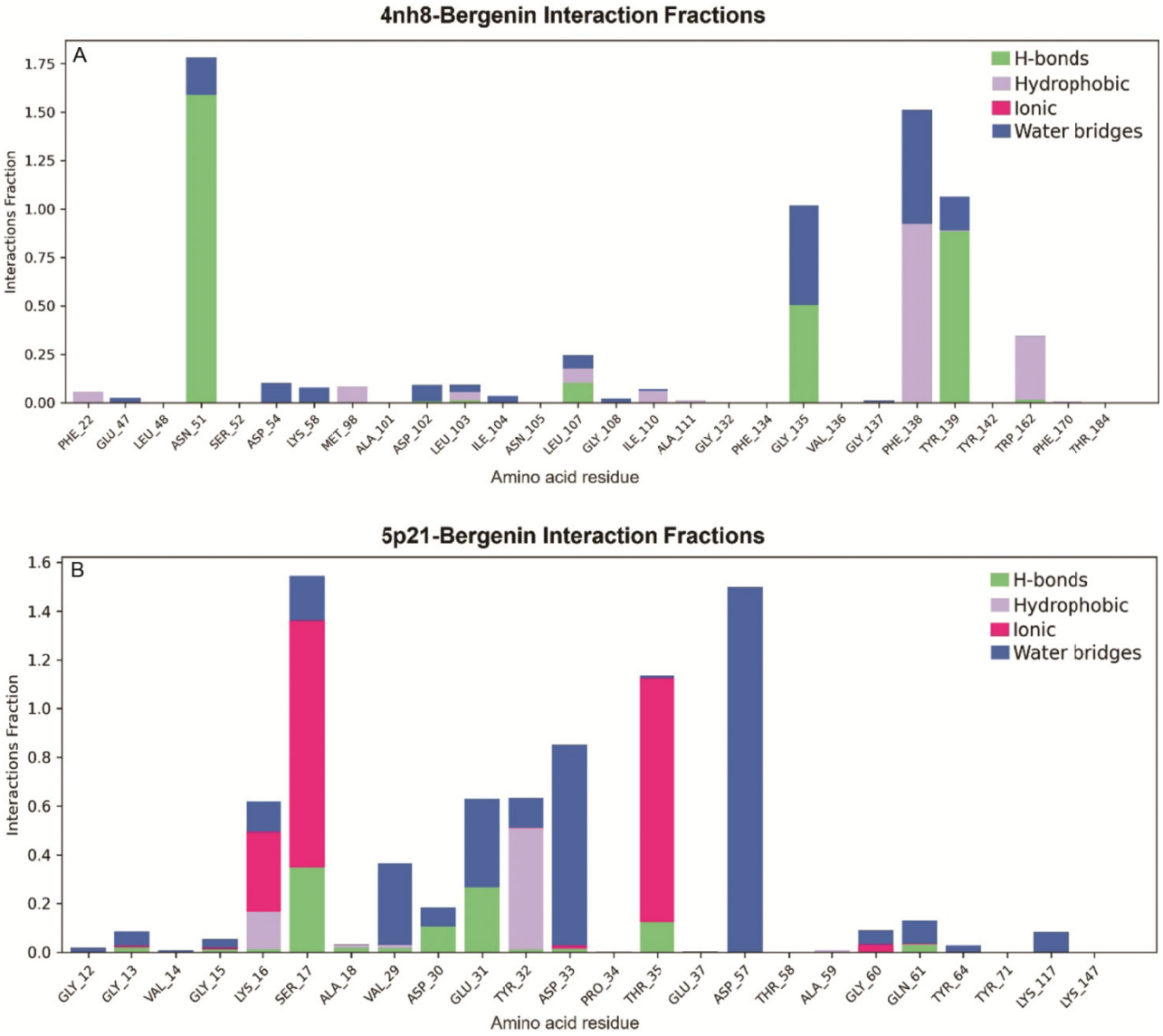

Fig. 9 — Protein Ligand interaction fractions of (A) 4nh8-Bergenin; and (B) 5p21-Bergenin

than 1.8 Å. In contrast, ligand contacts in the Bergenin-5p21 system as illustrated by green lines in (Fig. 8B), primarily observed with residues that fluctuated more compared to residues that were confined in rigid secondary conformations. Protein-ligand interactions of Bergenin-4nh8 and Begrenin-5p21 classified as Hydrogen Bonds, Hydrophobic, Ionic and Water Bridges were represented in (Fig. 9A & B, respectively). The plot in Figure 9A of Bergenin-4nh8 interaction fractions demonstrated the interacting amino acids Asn51, Leu107, Gly135, Phe138, Tyr139 and Trp162. Residues exposed to ligand preliminary by hydrogen bonds including Asn51 (1.59), Leu107 (0.1), Gly135 (0.5) and Tyr139 (0.88), with Asn51, Gly135 and Tyr139 additionally connecting to the ligand *via* water bridges, establishing interactions with water molecules. However, Phe138 (0.92) and Trp162 (0.33) shows hydrophobic interactions with Bergenin. Figure 9B for Bergenin-5p21 depicts the contribution of significantly interacting amino acids including Lys16, Ser17, Val29, Asp30, Glu31, Tyr32, Asp33, Thr35 and Asp57. However, relative significant interactions were showed by Ser17 (0.35), Asp30 (0.1), Glu31 (0.26) and Thr35 (0.13) residues in hydrogen bonds formation, while Lys16 (0.33), Ser17 (1.01) and Thr35 (1.0) exhibited ionic interaction. Both Lys16 (1.5) and Tyr32 (0.50) have Hydrophobic interactions whereas, water bridge formations are associated with several residues including Lys16,

Ser17, Val29, Asp30, Glu31 and Tyr32 with interaction fraction of 0.82 and 1.5 for Asp33 and Asp57 respectively. As demonstrated in Figure 10A, the interacting amino acid residues Asn51, Gly135, Phe138, and Tyr139 maintain persistent contact with the ligand over the 100 ns time scale. When Bergenin-5p21 was taken into consideration. Figure 10B illustrates the amino acid residues Ser17, Thr35 and Asp57 remained in stable

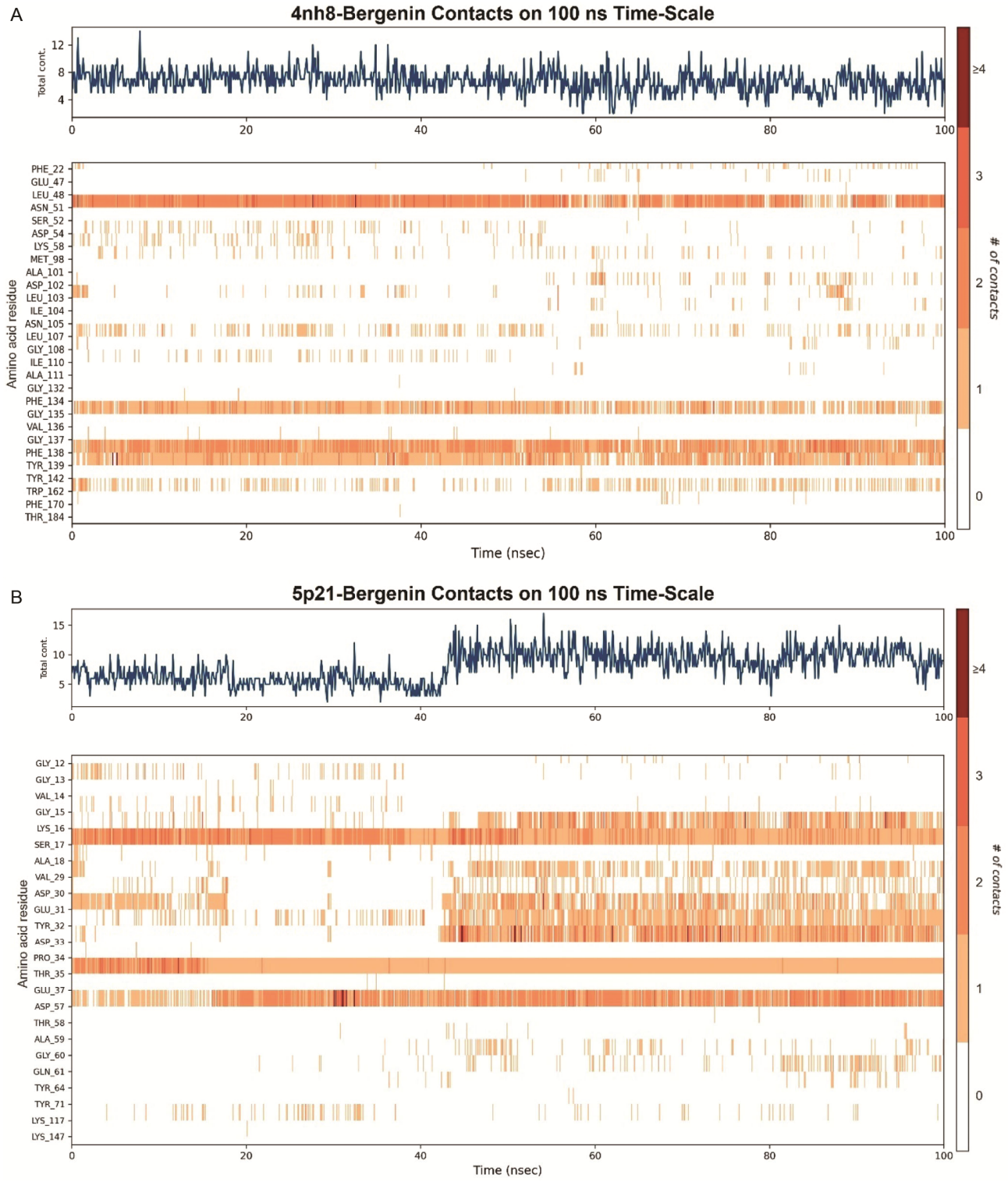

Fig. 10 — Protein Ligand contacts on 100 ns time scale of (A) 4nh8-Bergenin; and (B) 5p21-Bergenin

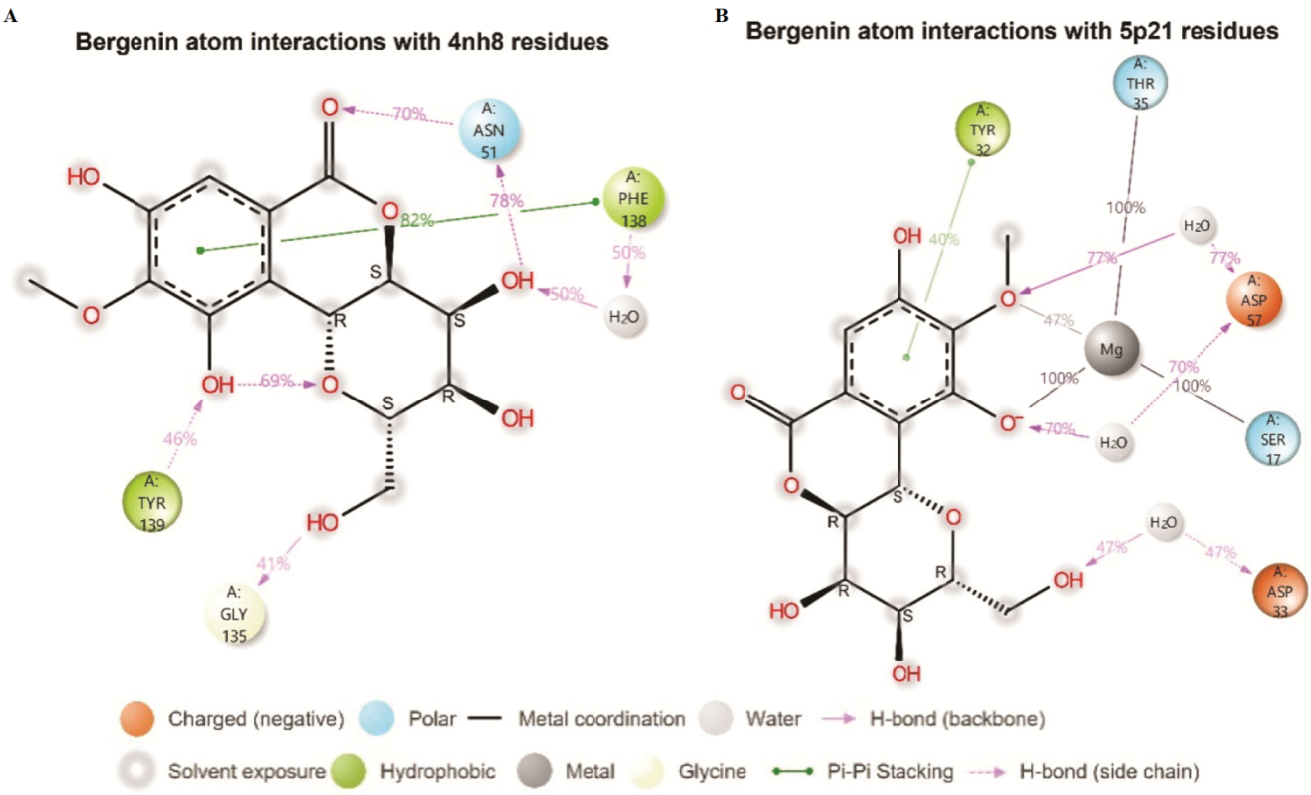

Fig. 11 — Ligand atom interactions with protein residues (A) Bergenin with 4nh8; and (B) Bergenin with 5p21

contacts throughout the 100 ns simulation period. After 40 ns, however, Lys16, Val29, Glu31, Tyr32 and Asp33 are responsible for the formation of new connections. These additional interactions help to stabilize the system after 40 ns, as reflected in Protein-ligand RMSD also. Significant connections exceeding a contact strength of 40% were detected in the schematic representation of ligand atom interactions with 4nh8 residues in (Fig. 11A). The amino acid residues Asn51, Gly135, Phe138, and Tyr139 create H-bonds with 78%, 41%, 50%, and 46% strength, respectively. Amongst these residues, hydrophobic residue Phe138 forms Pi-Pi stacking with an aromatic ring of Bergenin at 82% strength. Bergenin atomic interactions with 5p21 residues in (Fig. 11B) indicated that magnesium ion was engaged in metal coordination with Thr35 (100%) and Ser17 (100%). Tyr32 (40%) displays Pi-Pi stacking, whereas negatively charged amino acids Asp57 (70%) and Asp33 (47%), make contact through water bridges. These results suggested that Bergenin attained the stable docked conformation with 4nh8 and 5p21 during 100 ns simulation.

Discussion

Absorption Distribution Metabolism and Excretion (ADME) data is mostly used to determine if a chemical is suitable for usage as a medicine or whether a compound with pharmacological or biological activity may be developed into a human oral drug[25]. QikProp predicted, that ADME, pharmacokinetics and pharmacological properties of Bergenin have not violated any of the ADME criteria, satisfy Lipinski's rule of five and can be considered as a promising drug. Furthermore, Bergenin's low MDCK permeability and Blood/brain partition coefficient revealed that it was unable to pass the blood-brain barrier and therefore prevent possible toxicity. Next, potential protein targets based on probability scores, the ChEMBL, the Swiss target prediction, and the PharmMapper database (based on z' scores) stipulated 13, 23 and 232 probable targets respectively. A total of 268 targets were found that interact with Bergenin based on its chemical and pharmacological properties. Known breast cancer targets were extracted from GeneCards and PathCards to identify the correlation of Bergenin potential targets with Breast cancer. A list of intersection targets was created, which comprised both putative targets for Bergenin and known breast cancer. 234 overlapping targets were employed to create a protein-protein interaction (PPI) network based on the

STRING 11.5 database using Cytoscape 3.9.1 software. PPI network shows how target proteins interact with each other and contribute to various cell signaling pathways. MCODE and cytoHubba analysis of the aforementioned network revealed the key target proteins that play significant roles in the network. It also demonstrates that despite being a global-based strategy, degree, closeness, and MCC produced comparable outcomes. GO and KEGG enrichment analysis was performed using DAVID database to functionally annotates key target genes into main GO terms and KEGG pathway. GO enrichment reveals the main GO terms including biological processes, molecular functions, and cellular components *viz.*, GO:0007165 signal transduction, GO:0005515 protein binding, GO:0005829 cytosol *etc*. This implies that most of the target genes in the PPI network are found in the cytosol and take part in signal transduction and protein phosphorylation.

KEGG pathway enrichment analysis displayed pathways involved *viz.*, hsa05200: Pathways in cancer, hsa01100: Metabolic pathways, hsa04151: PI3K-Akt signaling pathway *etc*. According to GO and KEGG enrichment analysis, most of the target genes are expected to be involved in cancer metabolism and can be targeted to alter cell proliferation and cancer development. The CPDT complex network illustrates the enrichment of target genes depending on the KEGG pathways and gene-disease association. A CPDT was built using KEGG pathways and DisGeNET disease relatedness statistics analysis, which includes 20 nodes representing major KEGG pathways and 8 nodes being diseases, as well as 161 nodes representing key target genes (Fig. 5). cytoHubba evaluation of the PPI network for 161 target genes based on the scoring method of Degree, Closeness, MCC, Betweenness and BottleNeck exposed 10 prominent targets. SRC, HSP90AA1 and AKT1 were the common leading targets in the cytoHubba rank list. When it comes to scoring, SRC ranks first in all five categories, followed by HSP90AA1, AKT1, PIK3R1, HRAS and EGFR. Proteins encoded by these target genes were molecularly docked and subjected to ligand interaction analysis using Glide, Schrödinger. The molecular docking result in table 5 highlighted that Bergenin demonstrated superior binding interactions with these proteins compared to their respective FDA-approved inhibitors. The degree of interaction efficiency is reflected in the Glide scores, where Bergenin showed the highest efficiency when interacting with HSP90AA1 (-12.07), followed by HARS (-11.570), AKT1 (-9.954), EGFR (-9.585), PIK3R1 (-7.321) and SRC (-7.214). Similarly, molecular dynamics study demonstrated that Bergenin has a more stable docked structure with HSP90AA1 (4nh8) and HRAS (5p21). Bergenin with 4nh8 interaction data suggested that Asn51 and Phe138 continue to retain the characteristic hydrogen bond and Hydrophobic contact respectively throughout the 100 ns. Amino acid residues Asn51 and Phe138 are the ATP binding site of HSP90AA1[26]. Previously, similar binding models at this site of HSP90AA1 that operate as an inhibitor were described[27,28]. Therefore, binding of Bergenin at Asn51 and Phe138 may prevent the ATP binding and alter the activity of HSP90AA1 (Fig. 12).

Hsp90 alpha, encoded by HSP90AA1, is part of the Hsp90 family of proteins that works as a molecular chaperone. Hsp90 interacts with and supports several proteins that promote cancer cell survival, particularly in breast cancer[29]. As shown in Figure 12, Hsp90 stabilises oncoproteins such as AKT (PKB), which also stimulates autophagy and prevents apoptosis *via* the PI3K/Akt/mTOR pathway[30], implying that inhibiting HSP90AA1 might be a strategy for reducing cell proliferation and promoting apoptosis[31]. Hsp90 inhibitor sensitize cells with elevated levels of HER2 and AKT expression by inactivating AKT in both *in vitro* and *in vivo* models, indicating that Hsp90 inhibition downregulates AKT kinase and hence cell proliferation and induces apoptosis[32].

Equivalent results have been shown by Chen and colleagues in 2014 that the Hsp90 inhibitor promotes cell cycle arrest, destabilises tyrosine kinase; inhibits AKT activation and improves its antiproliferative effect on breast cancer[33]. Glide dock predicted Bergenin binds at kinase domain (spans 150-408 amino acids[34]) AKT forming hydrogen bonds with Glu278, Asn279, Glu298, and Phe293. Similar binding regions were explored by Mirza and Karim in 2023[35]. This suggests that the binding of Bergenin at the kinase domain could prevent activation (*i.e*., phosphorylation) of AKT. p-AKT, an active state of AKT, phosphorylates and inhibits p21 and p27 proteins[36] which are involved in cell cycle progression through inhibiting CDK-cyclin. It prevents apoptosis through the phosphorylation of FOXO, BAD and CASP9[37]. It is also controlled by SRC *via* PTEN and phosphorylation of PI3K[38].

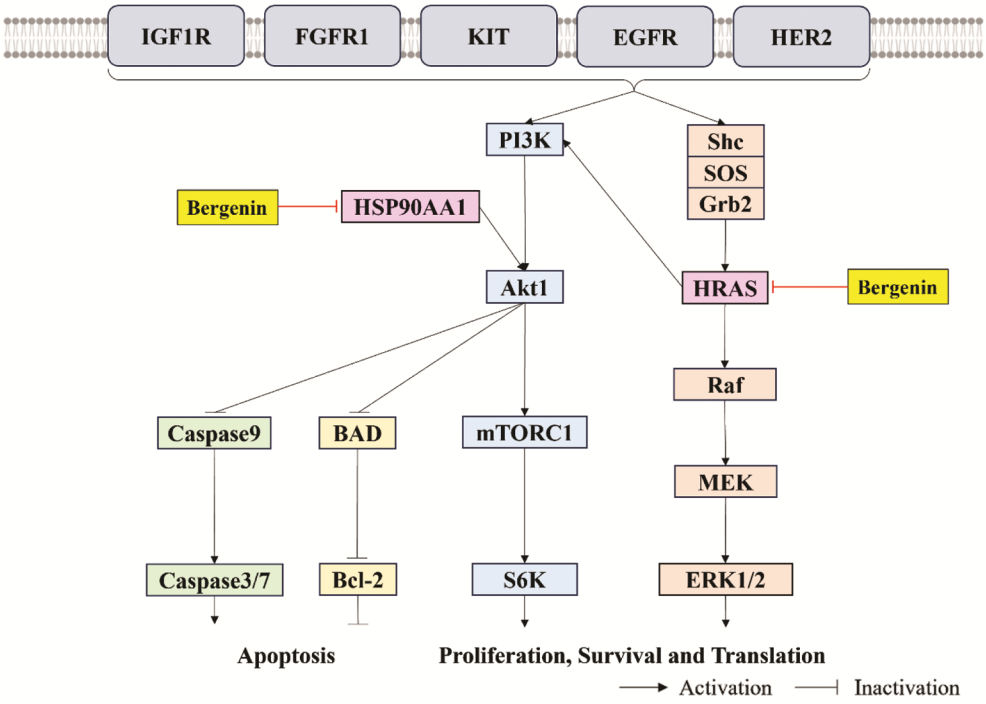

AKT1 = RAC-alpha serine/threonine protein kinase (protein kinase B (PKB)); BAD = Bcl-2 associated agonist of cell death; Bcl-2 = Apoptosis regulator Bcl-2 (B-cell lymphoma 2); Caspase3/7 and Caspase9 = Apoptotic proteins; EGFR = Epidermal growth factor receptor; ERK or MAPK3 = Extracellular signal regulated kinase 1; FGFR1 = Fibroblast growth factor receptor 1; Grb2 = Growth receptor bound protein; HER2 = Human epidermal growth factor receptor; HRAS = GTPase HRAS (p21 Ras); HSP90AA1 = Heat shock protein 90 alpha; IGF1R = Insulin like growth factor 1 receptor; KIT = proto-oncogene receptor tyrosine protein kinase; MEK or MAPKK (MAPK2) = Mitogen activated protein kinase kinase; mTORC1 = Serine/threonine protein kinase mTOR (Mammalian target of Rapamycin); PI3K = Phosphoinositide – 3 – Kinase; Raf = Raf-proto-oncogene serine/threonine protein kinase; RPS6K = Ribosomal protein s6 kinase; Shc = Shc transforming protein 1; SOS = Son of sevenless homolog.

Fig. 12 — Representation of the PI3K-Akt and MAPK pathways, emphasizing interaction of Bergenin with HSP90AA1 and HRAS to inhibit their activation. This interaction ultimately hinders the activation of AKT1 and Raf/MEK/ERK thereby promoting apoptosis and disrupting processes related to cancer cell proliferation, survival and translation

The HRAS (Harvey rat sarcoma viral oncogene homolog) gene encodes the Hras GTPase enzyme, which is activated by RTK type growth factor receptors. It acts as a binary switch that cycles between an inactive GDP-bound and an active GTP-bound state[39]. The active form of HRAS stimulates PI3K signaling and RAS-RAF-MEK-ERK pathway (Fig. 12) which further stimulates the expression of cyclin/CDKs promoting cell growth, proliferation and survival[40]. HRAS expressed in 60% of breast cancer patients and is also one of the most frequently altered oncogene families in cancer, impairing Ras responsiveness to GAP-mediated control and causing it to remain active[41]. Ras activation in breast cancer tumours can occur in the presence of EGFR or HER2 without a direct RAS mutation, accounting for 20-50% of cases. Elevated HRAS mRNA levels were most common in ER-positive breast cancer tumours[42]. The GTP binding site is represented by the amino acid residues Ser17, Thr35, and Asp57, which are implicated in the interaction of Bergenin with HRAS (5p21). Binding of Magnesium ions at this site is essential for HRAS activation *via* GTP hydrolysis. Till Rudack and colleagues in 2012[43] revealed the involvement of Mg^{++} ion in the catalysis of HRAS-GTP hydrolysis by providing transient storage of electrons, which is thereafter reversed by bond cleavage and Pi release[43]. Hence, interaction of Bergenin with amino acid residues and Mg^{++} ion at the GTP binding site of HRAS may inhibit its activation and, as a result, cell growth and division. A signaling pathway diagram in (Fig. 12) was constructed using the Breast cancer – KEGG pathway (map05224) as a reference which illustrates a potential mechanism of action for Bergenin. It highlights that by targeting HSP90AA1 and HRAS, Bergenin may effectively prevent the activation of AKT1 and RAF through the PI3K-Akt and MAPK signaling pathways respectively. This

action has the potential to promote apoptosis[44] and disrupt processes related to cancer cell proliferation, survival, and translation. Similar docking studies have previously demonstrated that phytocompounds have the potential to inhibit cancerous growth[45-48]. Therefore, targeting HSP90AA1 coupled with HRAS and AKT1 reduces cell viability and induces apoptosis and consequently, Bergenin might be a potential therapeutic drug to treat breast cancer.

Conclusion

The molecular mechanism of Bergenin, a bioactive phytochemical derived from *P. pterocarpum* flowers, in the therapy of breast cancer was investigated using network pharmacology and molecular docking in this study. Bergenin's potential primary targets for breast cancer have been found, and they include crucial pathway genes such as the PI3K-Akt pathway, the MAPK pathway, the EGFR pathway, and others. Key targets like HSP90AA1, HRAS and AKT1 showed the best Glide score when employed in molecular docking. MD simulation further validates the stable docked conformation of Bergenin with HSP90AA1 and HRAS. In a nutshell, Bergenin may lead to induction of apoptosis by disrupting processes related to cancer cell proliferation, survival *via* the PI3K-Akt and MAPK signaling pathway by targeting HSP90AA1, HRAS and AKT1.

Acknowledgment

Authors are thankful to the Council of Scientific & Industrial Research (CSIR), Ministry of Science and Technology, Government of India for providing financial assistance (Award no. - 09/0070(11301)/2021-EMR-I).

Conflict of interest

All authors declare no conflict of interest.

References

1 Sung H, Ferlay J, Siegel RL, Laversanne M, Soerjomataram I, Jemal A & Bray F, Global cancer statistics 2020: Globocan estimates of incidence and mortality worldwide for 36 cancers in 185 countries. *CA Cancer J Clin*, 71 (2021) 209.

2 Sathishkumar K, Vinodh N, Badwe RA, Deo SVS, Manoharan N, Malik R, Panse NS, Ramesh C, Shrivastava A, Swaminathan R, Vijay CR, Narasimhan S, Chaturvedi M & Mathur P, Trends in breast and cervical cancer in India under National Cancer Registry Programme: An Age-Period-Cohort analysis. *Cancer Epidemiol*, 74 (2021) 101982.

3 Partridge AH, Burstein HJ & Winer EP, Side effects of chemotherapy and combined chemohormonal therapy in women with early-stage breast cancer. *J Natl Cancer Inst*, 30 (2001) 135.

4 Hopkins AL, Network pharmacology: the next paradigm in drug discovery. *Nat Chem Biol*, 4 (2008) 682.

5 Zheng BB, Wang Q, Yue Y, Li J, Li XJ & Wang X, Network pharmacology and molecular docking validation to reveal the pharmacological mechanisms of kangai injection against colorectal cancer. *Biomed Res Int*, (2022) 3008842.

6 Sakle NS, More SA &Mokale SN, A network pharmacology-based approach to explore potential targets of *Caesalpinia pulcherima*: an updated prototype in drug discovery. *Sci Rep*, 10 (2020) 1.

7 Schrödinger Release 2023-3: Schrödinger, LLC, New York, NY, 2023.

8 Gaulton A, Hersey A, Nowotka ML, Patricia Bento A, Chambers J, Mendez D, Mutowo P, Atkinson F, Bellis LJ, Cibrian-Uhalte E, Davies M, Dedman N, Karlsson A, Magarinos MP, Overington JP, Papadatos G, Smit I & Leach AR, The ChEMBL database in 2017. *Nucleic Acids Res*, 45 (2017) 945.

9 Wang X, Shen Y, Wang S, Li S, Zhang W, Liu X, Lai L, Pei J & Li H, PharmMapper 2017 update: a web server for potential drug target identification with a comprehensive target pharmacophore database. *Nucleic Acids Res*, 45 (2017) 356.

10 Daina A, Michielin O & Zoete V, SwissTargetPrediction: updated data and new features for efficient prediction of protein targets of small molecules. *Nucleic Acids Res*, 47 (2019) 357.

11 Safran M, Rosen N, Twik M, BarShir R, Stein TI, Dahary D, Fishilevich S & Lancet D, The GeneCards Suite. *Practical Guide to Life Science Databases*, (2022) 27.

12 Szklarczyk D, Gable AL, Lyon D, Junge A, Wyder S, Huerta-Cepas J, Simonovic M, Doncheva NT, Morris JH, Bork P, Jensen LJ & Von Mering C, STRING v11: protein-protein association networks with increased coverage, supporting functional discovery in genome-wide experimental datasets. *Nucleic Acids Res*, 47 (2019) 607.

13 Bader GD & Hogue CW, An automated method for finding molecular complexes in large protein interaction networks. *BMC Bioinform*, 4 (2003) 2.

14 Chin CH, Chen SH, Wu HH, Ho CW, Ko MT & Lin CY, cytoHubba: identifying hub objects and sub-networks from complex interactome. *BMC SystBiol*, 8 (2014) 11.

15 The Gene Ontology resource: enriching a Gold mine. *Nucleic Acids Res*, 49 (2021) D325.

16 Kanehisa M, Furumichi M, Sato Y, Kawashima M & Ishiguro-Watanabe M, KEGG for taxonomy-based analysis of pathways and genomes. *Nucleic Acids Res*, 51 (2023) D587.

17 Sherman BT, Hao M, Qiu J, Jiao X, Baseler MW, Lane HC, Imamichi T & Chang W, DAVID: a web server for functional enrichment analysis and functional annotation of gene lists (2021 update). *Nucleic Acids Res*. 50 (2022) 216.

18 Piñero J, Ramírez-Anguita JM, Saüch-Pitarch J, Ronzano F, Centeno E, Sanz F & Furlong LI, The DisGeNET knowledge platform for disease genomics: 2019 update. *Nucleic Acids Res*, 48 (2020) 845.

19 Khan N, Johri S & Paul N, Inhibitory Activity of Polyphenolic Compound Extracted from P. Betel and T. Aestivum with Hepcidin for Iron Deficiency Anemia: An *in silico* approach. *Indian J Biochem Biophys*, 60 (2023) 485.

20 Repasky MP, Shelley M & Friesner RA, Flexible ligand docking with Glide. *Curr Protoc Bioinformatics*, 18 (2007) 36.

21 Jorgensen WL, Chandrasekhar J, Madura JD, Impey RW & Klein ML, Comparison of simple potential functions for simulating liquid water. *J Chem Phys,* 79 (1983) 926.

22 Martyna GJ, Klein ML & Tuckerman M, Nosé–Hoover chains: The canonical ensemble *via* continuous dynamics. *J Chem Phys,* 97 (1992) 2635.

23 Martyna GJ, Tobias DJ & Klein ML, Constant pressure molecular dynamics algorithms. *J Chem Phys,* 101 (1994) 4177.

24 Lipinski CA, Lombardo F, Dominy BW & Feeney PJ, Experimental and computational approaches to estimate solubility and permeability in drug discovery and development settings. *Adv Drug Deliv Rev,* 46 (2001) 3.

25 Guan M, Guo L, Ma H, Wu H & Fan X, Network pharmacology and molecular docking suggest the mechanism for biological activity of rosmarinic acid. *Evid Based Complement Altern Med,* (2021) 5190808.

26 The UniProt Consortium UniProt: The Universal Protein Knowledge base in 2023. *Nucleic Acids Res,* 51 (2023) 523.

27 Moon SJ, Jeong BC, Kim HJ, Lim JE, Kim HJ, Kwon GY, Jackman JA & Kim JH, Bruceantin targets HSP90 to overcome resistance to hormone therapy in castration-resistant prostate cancer. *Theranostics,* 11 (2021) 958.

28 Sain A, Khamrai D, Kandasamy T & Naskar D, Apigenin exerts anti-cancer effects in colon cancer possibly by regulating Heat shock protein 90 alpha family class A member 1 (HSP90AA1). *Biorxiv,* 3 (2023) 534119.

29 Zuehlke AD, Beebe K, Neckers L & Prince T, Regulation and function of the human HSP90AA1 gene. *Gene,* 570 (2015) 8.

30 Xiao X, Wang W, Li Y, Yang D, Li X, Shen C, Liu Y, Ke X, Guo S & Guo Z, HSP90AA1-mediated autophagy promotes drug resistance in osteosarcoma. *J Exp Clin Cancer Res,* 37 (2018) 201.

31 Ren X, Li T, Zhang W & Yang X, Targeting heat-shock protein 90 in cancer: an update on combination therapy. *Cells,* 11 (2022) 2556.

32 Niu M, Zhang B, Li L, Su Z, Pu W, Zhao C, Wei L, Lian P, Lu R, Wang R, Wazir J, Gao Q, Song S & Wang H, Targeting HSP90 inhibits proliferation and induces apoptosis through AKT1/ERK pathway in lung cancer. *Front Pharmacol,* 12 (2022) 4113.

33 Chen SM, Guo CL, Shi JJ, Xu YC, Chen Y, Shen YY, Su Y, Ding J & Meng LH, HSP90 inhibitor AUY922 abrogates up-regulation of RTKs by mTOR inhibitor AZD8055 and potentiates its antiproliferative activity in human breast cancer. *Int J Cancer,* 135 (2014) 2462.

34 Pérez-Tenorio G, Karlsson E & Stål O, Clinical value of isoform-specific detection and targeting of AKT1, AKT2 and AKT3 in breast cancer. *Breast Cancer Manag,* 3 (2014) 409.

35 Mirza Z & Karim S, Structure-based profiling of potential phytomolecules with AKT1 a key cancer drug target. *Molecules,* 28 (2023) 2597.

36 Manning BD & Toker A, AKT/PKB Signaling: Navigating the network. *Cell,* 169 (2017) 381.

37 Chen YH, Li CL, Chen WJ, Liu J & Wu HT, Diverse Roles of FOXO Family Members in Gastric Cancer. *World J Gastrointest Oncol,* 13 (2021) 1367.

38 Shan KS, Rios AB, Theik NWY, Hussein A & Blaya M, Molecular Targeting of the Phosphoinositide-3-Protein Kinase (PI3K) Pathway Across Various Cancers. *Int J Mol Sci,* 25 (2024) 1973.

39 Galiè M, RAS as supporting actor in breast cancer. *Front Oncol,* 9 (2019) 1199.

40 Yang J, Nie J, Ma X, Wei Y, Peng Y & Wei X, Targeting PI3K in cancer: mechanisms and advances in clinical trials. *Mol Cancer,* 18 (2019) 1.

41 Banys-Paluchowski M, Milde-Langosch K, Fehm T, Witzel I, Oliveira-Ferrer L, Schmalfeldt B & Müller V, Clinical relevance of H-RAS, K-RAS, and N-RAS mRNA expression in primary breast cancer patients. *Breast Cancer Res Treat,* 179 (2020) 403.

42 Eckert LB, Repasky GA, Ülkü AS, McFall A, Zhou H, Sartor, CI & Der CJ, Involvement of Ras activation in human breast cancer cell signaling, invasion, and anoikis. *Cancer Res,* 64 (2004) 4585.

43 Rudack T, Xia F, Schlitter J, Kötting C & Gerwert K, The role of magnesium for geometry and charge in GTP hydrolysis, revealed by quantum mechanics/molecular mechanics simulations. *Biophys J,* 103 (2012) 293.

44 Sandra F, Suryajaya K, Chouw A, Celinna M, Ranggaini D, Lee KH & Sartika CR, *Eleutherine bulbosa* bulb extract induces apoptosis and inhibits cell migration by downregulating Sonic hedgehog in human tongue cancer cells: An *in vitro* study. *Indian J Biochem Biophys*, 60 (2023) 763.

45 Barukial P, Ahmed B, Singha B, Chetia P, Das NK, Thakur S, Sinha UB & Bezbaruah B, Some Co (II)-schiff base complexes as promising anticancer agents: A DFT and Molecular docking study. *Indian J Biochem Biophys*, 61 (2024) 354.

46 Latha V, Gomathi V, Rajeshkanna A & Hari Ram S, Generating a potent inhibitor against MCF7 breast cancer cell through artificial intelligence based virtual screening and molecular docking studies. *Indian J Biochem Biophys*, 60 (2023) 844.

47 Agarwal T, Manivannan HP, Gayathri R, Veeraraghavan VP, Sankaran K & Francis AP, Selective plant alkaloids as potential inhibitors of PARP in pancreatic cancer-An *in silico* study. *Indian J Biochem Biophys,* 60 (2023) 555.

48 Kiewhuo K, Jamir E, Priyadarsinee L, Nagamani S & Sastry GN, Screening of phytochemicals for potential breast cancer targets BRCA1 and BARD1: A network pharmacology approach. *Indian J Biochem Biophys*, 60 (2023) 393.